Modifications of magnetic anisotropy and magnetization reversal in [Co0.4nm/Pd0.7 nm]50 multilayers induced by 10keV-He ion bombardment

Arno Ehresmann, Olav Hellwig, Oliver Buhl, Nicolas David Müglich, Tanja Weis, and Dieter Engel

Citation: Journal of Applied Physics **112**, 063901 (2012); doi: 10.1063/1.4752274
View online: http://dx.doi.org/10.1063/1.4752274
View Table of Contents: http://scitation.aip.org/content/aip/journal/jap/112/6?ver=pdfcov
Published by the AIP Publishing

Modifications of magnetic anisotropy and magnetization reversal in $[Co^{0.4\,nm}/Pd^{0.7\,nm}]_{50}$ multilayers induced by 10 keV-He ion bombardment

Arno Ehresmann,[1,a)] Olav Hellwig,[2] Oliver Buhl,[1] Nicolas David Müglich,[1] Tanja Weis,[1] and Dieter Engel[1]
[1]*Institute of Physics and Center for Interdisciplinary Nanostructure Science and Technology (CINSaT), University of Kassel, Heinrich-Plett-Strasse 40, Kassel 34132, Germany*
[2]*San Jose Research Center, HGST, A Western Digital Company, 3403 Yerba Buena Road, San Jose, California 95135, USA*

(Received 2 July 2012; accepted 9 August 2012; published online 17 September 2012)

$[Co^{0.4\,nm}/Pd^{0.7\,nm}]_{50}$ multilayers with Pd film thicknesses in the first ferromagnetic maximum of interlayer exchange coupling display almost purely perpendicular-to-plane anisotropy and labyrinth stripe domain patterns in remanence. Their magnetization reversal is characterized by domain nucleation starting at a defined field H_N and domain wall movement in a defined magnetic field range. The modification of the magnetization reversal by 10 keV He ion bombardment due to the reduced magnetic anisotropy has been investigated by polar magneto-optical Kerr effect, by vibrating sample magnetometry, and by magnetic force microscopy at room temperature. It is shown that the ion bombardment creates and increases areas with ferromagnetic in-plane anisotropy and proportions of the sample showing superparamagnetism, the latter predominantly in the deeper layers. © *2012 American Institute of Physics*. [http://dx.doi.org/10.1063/1.4752274]

I. INTRODUCTION

The large variety of magnetic domain patterns observed in magnetic layer systems or multilayers is a consequence of the competition between several energy terms, specific to each layer system. These domain patterns may display the formation of multiple phases or mesoscopic order.[1] Accordingly, for a set layer system, a varying external field changes the domain pattern and results in a specific magnetization reversal. These characteristic features of magnetic layer systems (domain patterns, magnetization reversal) are intimately connected to the material system and its deposition parameters which essentially determine the contributing energies. External stimuli like varying temperature, pressure, or an external magnetic field may change these parameters reversibly or irreversibly (when diffusion processes or structural changes are involved). A versatile method to change magnetic layer characteristics after layer deposition is bombardment by ions, where ions deposit energy in the layer system, create defects, or are implanted. Whereas fluencies of heavy ions have to be very low to achieve a defined layer modification without destroying the thin layers by sputtering, light ions may be used up to intermediate fluencies due to their low sputter yields. Light-ion bombardment allows therefore tailoring of magnetic anisotropies[2–9] by inducing defects within the layers or at interfaces with almost no sputter effects. The deposited energy and the induced defects, however, will change usually more than one of the energies contributing to the total energy of the system and the resulting effects will be governed by a delicate balance between the modified anisotropy terms. Therefore, it is essential to understand the effects of light ion bombardment on magnetic thin film systems, when it is used for a deliberate anisotropy tailoring.

In the present paper, the modification of the domain pattern and magnetization reversal of $[Co^{0.4\,nm}/Pd^{0.7\,nm}]_{50}$ multilayers by 10 keV He ion bombardment will be investigated by polar Kerr magnetometry (p-MOKE), vibrating sample magnetometry (VSM), and magnetic force microscopy (MFM). This multilayer system has been chosen due to its particularly rich domain structure,[1] changing, e.g., with the number of Co/Pd bilayer repetitions. For the number of bilayer repetitions investigated here, a labyrinth domain pattern with domain sizes of about 100 nm is expected[1] and magnetization reversal is expected to occur over a field range of about 400 kA/m.

II. SAMPLE PREPARATION AND CHARACTERIZATION

The thin film system consisted of a magnetron sputter deposited $[Co^{0.4\,nm}/Pd^{0.7\,nm}]_{50}$ multilayer on 5 nm Pd buffer. Substrates were Si wafers with natural oxide. $[Co^{0.4\,nm}/Pd^{1.5\,nm}]$ was used as a cap bilayer to prevent oxidation of the ferromagnetic films (Fig. 1). The thickness of the Pd films in the multilayer had been chosen to induce ferromagnetic interlayer exchange coupling.[1] After deposition, this multilayer has been characterized by different methods: Fig. 2(a) shows the result of a p-MOKE measurement, Fig. 2(b) characterization by VSM sensitive to the perpendicular-to-plane (pp-sensitive) magnetization component $M_\perp$, and Fig. 2(c) VSM measurements sensitive to the in-plane (ip-sensitive) magnetization component M_{II}. The results of both characterization measurements for $M_\perp$ (Figs. 2(a) and 2(b)) are consistent and display the following distinct features of a fully antisymmetrical hysteresis loop, characteristic for magnetic thin films with perpendicular anisotropy:[1,10–12] Reducing H from large positive values towards 0, the magnetization stays essentially

a)Electronic address: ehresmann@physik.uni-kassel.de.

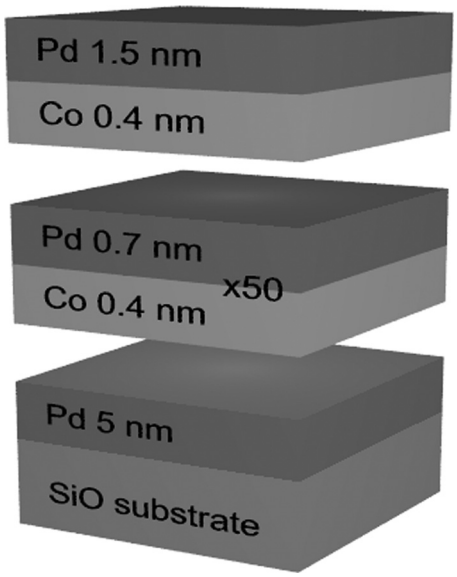

FIG. 1. Sketch of the investigated multilayer system.

saturated for the perpendicular magnetization component down to a particular field H_N, where domain nucleation starts.

The following steep decrease of $M_\perp$ with decreasing magnetic field indicates the magnetic field range where domain nucleation dominates (dashed in Fig. 2(a), i.e., rapid magnetization rotation in a larger number of distinct small areas. Domain nucleation is followed by a field range ΔH_W, where an almost linear, less steep change in magnetization is observed, which indicates a widening of domains on expense of those with the antiparallel magnetization direction (dotted in Fig. 2(a)). When all domains join, they annihilate at H_A, the annihilation field, corresponding again to magnetic saturation. From Figs. 2(a) and 2(b), no indication for coherent magnetization rotation can be inferred. On the backward branch, with increasing magnetic field, the same features are obvious: a nucleation starting at a field H_N' and a linear range of magnetization reversal by domain wall movement until positive saturation is reached at H_A', where all domains have annihilated (dashed quantities not marked in Fig. 2). The ip-sensitive VSM loop of Fig. 2(c) displays essentially a hard magnetic axis with an almost negligible ferromagnetic proportion. Therefore, the investigated sample possesses almost exclusively perpendicular-to-plane anisotropy with an extremely small contribution of in-plane anisotropy. This indicates the excellent thickness homogeneity of the Co layers at 0.4 nm, since Co layers with somewhat smaller thicknesses display a sharp transition from ferromagnetic to superparamagnetic behaviour.[13] The characteristic quantities of the loops together with the average slopes of the linear ranges within ΔH_W (forward branch, marked by a red line in Fig. 2(b)) and $\Delta H_W'$ (backward branch, marked by a blue line in Fig. 2(b)) are listed in Table I. Uncertainties for the magnetic field determination within the p-MOKE measurements is essentially determined by the distance between data points (1 data point per 36 kA/m with an individual uncertainty of ±4 kA/m) and similarly for the VSM measurements

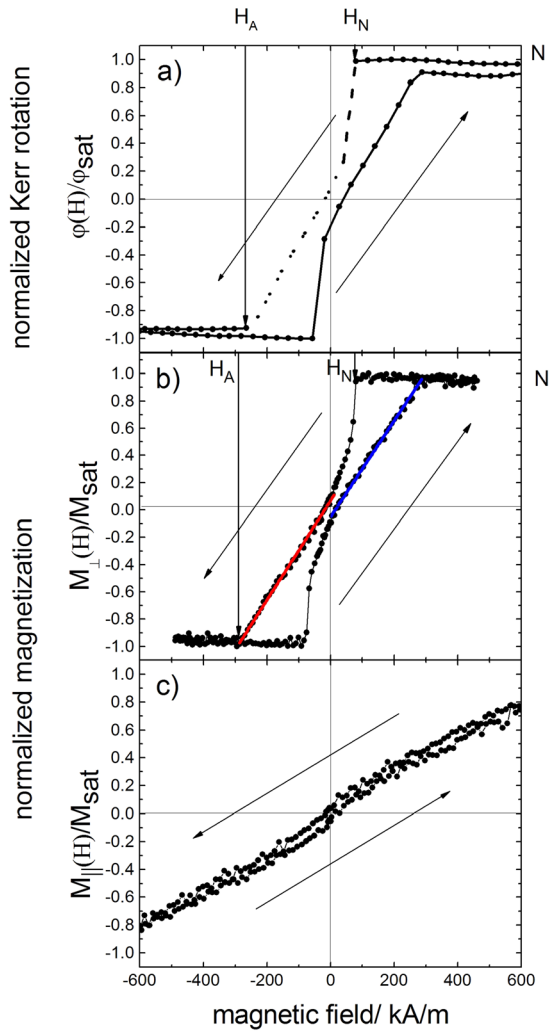

FIG. 2. (a) Hysteresis loop of the layer system prior to ion bombardment recorded by p-MOKE. Marked fields are H_N (domain nucleation field) and H_A (domain annihilation field). The marked normalized Kerr rotation N is the Kerr rotation prior to domain nucleation. (b) Characterization by pp-sensitive VSM. The linear ranges H_W in the forward and H_W' in the backward branch corresponding to domain widening are marked by a red and a blue line, respectively. (c) ip-sensitive VSM characterization. All measurements have been carried out at room temperature.

(1 data point per 6.6 kA/m with an individual uncertainty of ±0.8 kA/m). Uncertainties for the normalized magnetization values are determined by the scatter of the data in magnetic saturation and uncertainties due to instrument calibration and amount to 0.015 for the VSM and 0.012 for the p-MOKE measurements.

From Figs. 2(a) and 2(b), it is clear that the domain pattern has already nucleated at $H_{ext} = 0$. It has, therefore, been imaged prior to bombardment in remanence at room temperature by magnetic force microscopy (MFM). Fig. 3 shows an image with average stripe widths of 150 ± 30 nm (black stripes) and of 129 ± 17 nm (white stripes), determined by the average full width at half maximum of the peaks and dips of line scans similar to the one indicated by the white line in Fig. 3. The dark stripes are wider than the white stripes, being characteristic for the remanent magnetization perpendicular to plane seen in Figs. 2(a) and 2(b). The ratio of the stripe widths correspond to the expected ratio of up/

TABLE I. Magnetic characteristics of the measured pp-sensitive hysteresis loops. Uncertainties of magnetic field values for the p-MOKE measurements are ±18 kA/m, for the VSM measurements ±3.3 kA/m due to the measurement point density.

Fluence (ions/cm^2)	H_N (H_N') (kA/m)	H_A (H_A') (kA/m)	N (N′)	$\frac{\Delta^\varphi/_{\varphi_{sat.}}}{\Delta H}\left(\frac{\Delta^\varphi/_{\varphi_{sat.}}}{\Delta H}^{I}\right)$ (10^{-4} m/kA)	ΔH_W ($\Delta H_W'$) (kA/m)
p-MOKE					
Prior to IB	79 (−57)	−265 (288)	0.99 (−1.00)	38.4 ± 1.7 (38.5 ± 1.5)	112 (112)
1×10^{13}	116 (−93)	−265 (288)	0.99 (−0.91)	38.2 ± 1.3 (38.1 ± 1.7)	112 (112)
1.1×10^{14}	152 (−131)	−265 (290)	0.98 (−1.00)	31.9 ± 1.8 (34.1 ± 1.5)	148 (157)
2.2×10^{14}	152 (−130)	−266 (287)	0.70 (−0.69)	27.9 ± 1.5 (27.9 ± 1.4)	232 (232)
4.2×10^{14}	191 (−170)	−266 (287)	0.67 (−0.69)	25.9 ± 0.8 (25.9 ± 0.8)	233 (232)
VSM (pp-sensitive)					
Prior to IB	79 (−84)	−286 (281)	0.94 (−0.96)	36.4 ± 0.4 (34.2 ± 0.5)	301 (292)
1×10^{13}	84 (−85)	−285 (281)	0.72 (−0.70)	30.4 ± 0.5 (30.8 ± 0.4)	340 (341)
1.1×10^{14}	148 (−144)	−283 (288)	0.60 (−0.64)	26.2 ± 0.4 (25.5 ± 0.4)	205 (197)
2.2×10^{14}	159 (−159)	−299 (304)	0.83 (−0.83)	31.3 ± 0.2 (31.2 ± 0.2)	231 (228)
3.2×10^{14}	166 (−167)	−318 (327)	0.75 (−0.74)	28.7 ± 0.2 (29.3 ± 0.2)	262 (261)
4.2×10^{14}	177 (−174)	−315 (320)	0.75 (−0.72)	26.8 ± 0.2 (27.4 ± 0.2)	305 (309)

down magnetized areas inferable from Figs. 2(a) and 2(b). Although low magnetic moment tips have been used, an influence of the magnetized tip on the domain pattern cannot be completely excluded (this would lead to a widening of the black areas of Fig. 3 and a narrowing of the white areas).

III. MODIFICATION BY ION BOMBARDMENT

After magnetic characterization of the layer system, the sample has been bombarded homogeneously by 10 keV-He^+-ions in subsequent fluence steps as indicated in Tables I and II. Fig. 4 shows corresponding p-MOKE, Fig. 5 pp-sensitive, and Fig. 6 ip-sensitive VSM hysteresis loops. In the following, we discuss the effects of ion bombardment by the fluence dependences of the different magnetic characteristics of the sample.

A. Magnetization for fields larger than $|H_N|$ and magnetization N at H_N

Prior to bombardment, the sample displayed almost exclusively perpendicular-to-plane anisotropy with magnetization reversal starting with domain nucleation at magnetic saturation. As seen in Figs. 2(a) and 2(b), $M_\perp$ stays at saturation down to H_N. The ip-sensitive loop (Fig. 2(c)) displays a linear change of the in-plane magnetization component M_{II} with essentially negligible hysteresis. Such magnetic field dependence of the magnetization is characteristic for a magnetic hard direction with a very small ferromagnetic contribution with in-plane anisotropy or for superparamagnetic behaviour with small arguments of the characteristic Langevin function (see below). M_{II} contributes only negligibly to the total magnetization of the sample prior to bombardment, since no decrease of $M_\perp$ with decreasing magnetic field in the pp-sensitive loops at fields $H > |H_N|$ is observed within the uncertainties of the measurements.

Already for the lowest applied fluence, the ip-sensitive VSM measurement shows a noticeable increase of the hysteretic contribution to the in-plane magnetization component reversal curve (Fig. 6(a)), indicating an increasing proportion of the sample with ferromagnetic in-plane anisotropy. This part is seen in the pp-sensitive VSM measurements (Fig. 5(a)) as a hard axis contribution with an approximately linear decrease of $M_\perp$ from higher fields towards H_N. For the

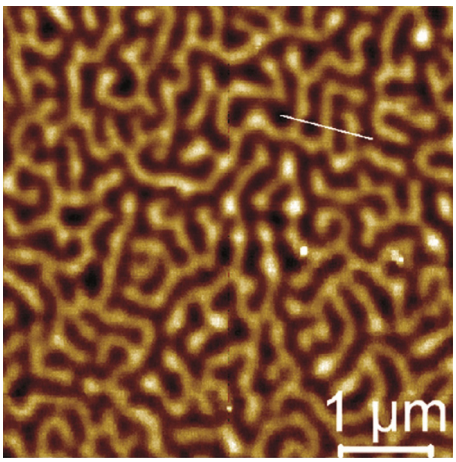

FIG. 3. MFM image of the sample prior to ion bombardment.

TABLE II. Results of the fits to the recorded ip-sensitive VSM hysteresis loops as a function of the ion fluence. Fit parameters a, b, c, and d are as in Eq. (1). a is a measure for the hard magnetic contribution to the in-plane component of the magnetization, b is a measure for the superparamagnetic contribution to the in-plane magnetization component relative to the ferromagnetic (easy) contribution, and c describes the average number of magnetic moments in the superparamagnetic Co clusters in Bohr magnetons. d describes the ferromagnetic easy contribution to the in-plane magnetization component.

Fluence (10^{13} ions/cm^2)	a (1/(A/m))	b	c	d
1	7.9×10^{-4}	0.34	2282	0.10
11	7.4×10^{-4}	0.39	3457	0.08
22	6.1×10^{-4}	0.45	4266	0.11
32	1.6×10^{-4}	0.75	3360	0.18
42	1.4×10^{-7}	0.84	2979	0.25

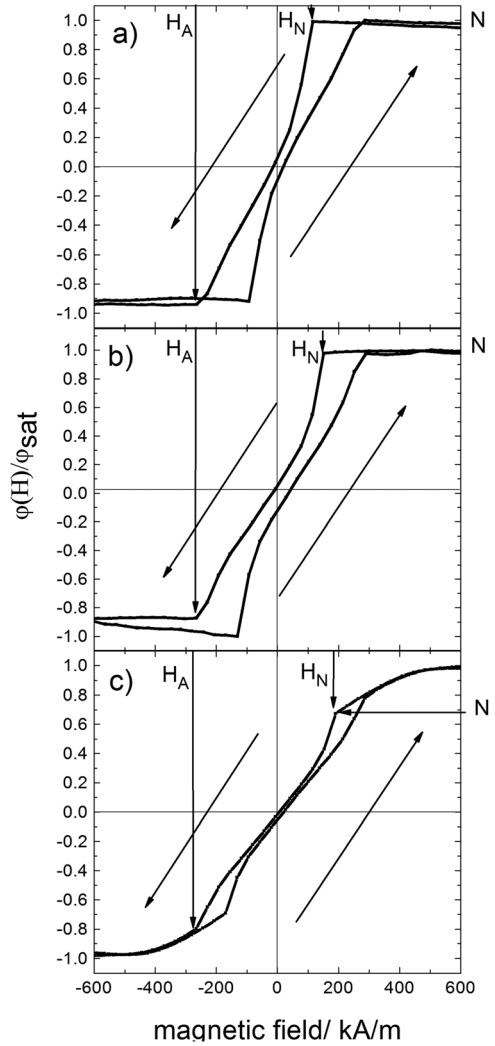

FIG. 4. p-MOKE hysteresis loops after 10 keV-He^+ ion bombardment by selected fluences. Marked quantities are as in Fig. 1. (a) 1.0×10^{13} ions/cm^2, (b) 1.1×10^{14} ions/cm^2, (c) 4.2×10^{14} ions/cm^2.

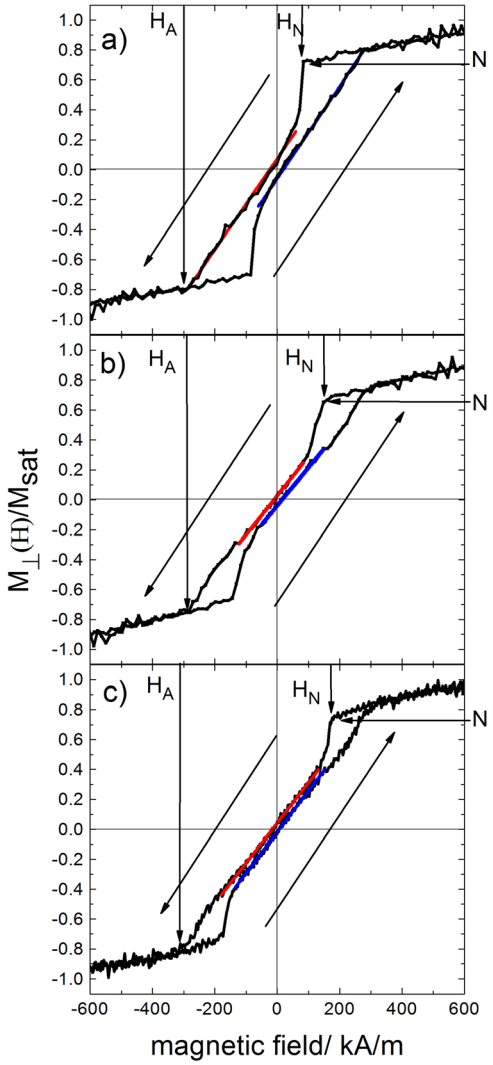

FIG. 5. pp-sensitive VSM hysteresis loops after ion bombardment. (a) 1.0×10^{13} ions/cm^2, (b) 1.1×10^{14} ions/cm^2, (c) 4.2×10^{14} ions/cm^2.

higher fluencies, a rounded loop in the ip-sensitive VSM data is observable, characteristic for an additional superparamagnetic proportion of the film system, which leads to a further reduction of the magnetization at H_N and H_N' from the saturation value. Co layers with thicknesses smaller than 0.4 nm usually display superparamagnetic behaviour, since at these thicknesses, the films are no more continuous and consist of separate superparamagnetic grains. The thickness of the Co films in the presently investigated sample has been just above this critical thickness. The ion bombardment causes defects and diffusion leading to a gradual disruption of the continuous layers into superparamagnetic grains. Therefore, the recorded ip-sensitive VSM data have been fitted by a model function, which accounts for a hard and soft in-plane ferromagnetic contribution and a superparamagnetic portion of the films

$$M_{II}/M_S(H) = a \times H + b \times \left(\frac{\cos h(c \times 2.816 \times 10^{-6} \times H)}{\sin h(c \times 2.816 \times 10^{-6} \times H)} - \frac{1}{c \times 2.816 \times 10^{-6} \times H} \right) \pm d. \quad (1)$$

In Eq. (1), the first term (fit parameter a) accounts for the hard magnetic contribution to the in-plane component of the magnetization, the second term describes the superparamagnetic part of the layer system, where parameter b is a measure for the superparamagnetic contribution to the in-plane magnetization component relative to the ferromagnetic (easy) contribution and c describes the average number of magnetic moments in the superparamagnetic Co clusters in Bohr magnetons. The third term (fit parameter d) describes the ferromagnetic easy contribution to the in-plane magnetization component, which is added or subtracted from the measured signal, depending on the branch of the hysteresis loop. Fits have been carried out for all ip-sensitive VSM hysteresis loops for field ranges between 200 A/m and maximum field of the measurements. The results of the fits have been included in Fig. 6 and the obtained parameters are shown in Table II as a function of the ion fluence. The ip-sensitive data prior to bombardment have been excluded from the fits, since for this data, it is not possible to distinguish between the magnetic hard and the superparamagnetic contribution due to the linear behaviour of the data even for fields $H > |H_N|$ (for small arguments, the Langevin function can be

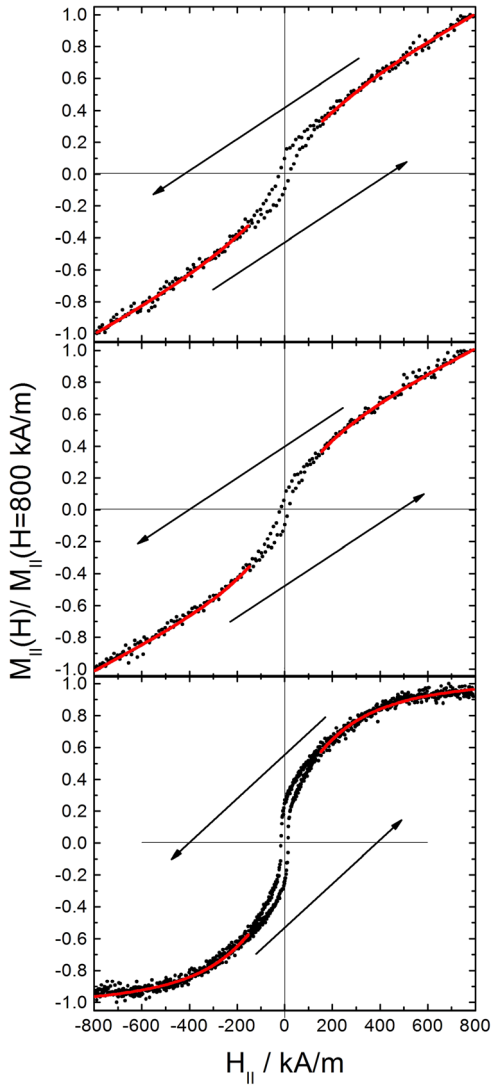

FIG. 6. ip-sensitive VSM hysteresis loops after ion bombardment. (a) 1.0×10^{13} ions/cm^2, (b) 1.1×10^{14} ions/cm^2, (c) 4.2×10^{14} ions/cm^2. Dots = measured data. Red lines = fits by Eq. (1) and fit parameters of Table I.

approximated by a linear function). The rounded shape of the curves, however, for the bombarded samples enabled distinction between these two contributions by the fits.

As is obvious from Table II, the magnetic hard contribution to the in-plane magnetization component is decreasing with increasing ion fluence. Such a behaviour can be expected due to the gradual reduction of the perpendicular-to-plane anisotropy of the layer system, which manifests itself as a hard contribution in the in-plane component. On the other hand, the ferromagnetic part with easy plane anisotropy is increasing with increasing ion fluence as well as the superparamagnetic part. Table I nicely displays the anisotropy changes of the layer system from a system with essentially perpendicular-to-plane anisotropy to a system with mainly superparamagnetic behaviour and some ferromagnetic in-plane contribution.

The superparamagnetic behaviour is particularly obvious in the pp-sensitive and ip-sensitive VSM measurements rather than in the p-MOKE ones. This can be explained by the fact that the VSM measurements are sensitive to the magnetization contribution of the whole layer stack, whereas the sensitivity of the p-MOKE with laser wavelength of 632 nm decreases with increasing depth of the layers. Light ion bombardment causes defects predominantly at the end of their trajectories in the layer system, i.e., in the deeper layers. The contribution of these layers to the signal is more prominent in the VSM measurements, less in the p-MOKE signals.

B. Nucleation field H_N

From Table I and Figs. 4 and 5, it is obvious that the nucleation fields are increasing with increasing ion fluencies. This is explainable by an increasing density of pinning sites due to the increasing ion bombardment induced defect density in the layer system. Within the uncertainties of the measurements, nucleation fields H_N and H_N' are increasing symmetrically with respect to 0 applied magnetic field.

C. Magnetic field ranges of nucleation and domain widening

Prior to ion bombardment magnetization, reversal starts at H_N with nucleation of domains followed by domain widening, indicated by a linear change of M with H (see ΔH_W in Table I). This linear range extends to the annihilation field, i.e., domains annihilate through widening and joining each other. This changes upon the 10 keV He^+ ion bombardment. For increasing ion fluencies, two effects are observed: (1) The linear range of magnetization reversal stops to continue to the annihilation field. For magnetic fields slightly lower than H_A, the slope of the magnetization reversal curve becomes steeper, indicating an additional mechanism for magnetization reversal. Since that part of the graph is similar to the one characteristic for domain nucleation, this seems to be the additional mechanism. (2) The slopes of the loops have been determined by differentiating the graphs. The linear range can then be identified by a constant slope as a function of H, which decreases with increasing ion fluence. Therefore, domains widen less fast with varying perpendicular-to-plane magnetic field with increasing ion fluence. This is understandable by the gradual reduction of the perpendicular-to-plane magnetic anisotropy due to the ion bombardment. Also an increase in defect density may not allow a completely free domain propagation. The linear range associated to domain widening shrinks with increasing ion fluence.

D. Annihilation field H_A

The annihilation fields determined by the p-MOKE and pp-sensitive VSM measurements are also symmetric with respect to $H = 0$. From the pp-sensitive VSM results (with less uncertainties), an increase of the annihilation field is observed. The reason for this increase might be again an increase in defect density, causing an increase of pinning sites and a decrease of the perpendicular anisotropy.

E. Superparamagnetic behaviour

The nonlinear approach of magnetic sample saturation in Figs. 5(c) and 6(c) indicate proportions of the layers with

superparamagnetic behaviour. As has been described above, the graphs of Fig. 6 have been fitted by Eq. (1). As is obvious from the results displayed in Table II, the superparamagnetic proportion of the multilayer system increases upon increasing ion dose (parameter b in Table II). The fit also indicates a characteristic change in the average number of magnetic moments in the superparamagnetic clusters, which first increases and at higher fluencies decreases. A possible explanation might be that small applied ion doses will separate the initially continuous Co layers into larger superparamagnetic clusters. Application of larger ion doses will induce more interdiffusion and defects leading to smaller superparamagnetic Co clusters.

IV. CONCLUSION

The 10 keV He^+ ion bombardment induced modification of sputter deposited $[Co^{0.4\,nm}/Pd^{0.7\,nm}]_{50}$ multilayers with Pd film thicknesses in the first ferromagnetic maximum of interlayer exchange coupling has been investigated by p-MOKE magnetometry, pp- and ip-sensitive VSM magnetometry, and magnetic force microscopy. Prior to bombardment, these samples display almost purely perpendicular-to-plane anisotropy and labyrinth domain patterns in remanence. Their magnetization reversal is characterized by domain nucleation starting at a defined field H_N and domain widening in a defined magnetic field range. 10 keV He ion bombardment with increasing fluencies reduces gradually the anisotropy of the film system resulting in a multitude of changes in the magnetic characteristics of the sample: (1) Proportions with in-plane anisotropy or showing superparamagnetism are created or increased with increasing fluence. (2) The number of pinning sites for domain nucleation increases or the perpendicular anisotropy constant decreases with increasing fluence and, therefore, the nucleation field increases. (3) Domain widths in remanence increase with increasing fluence. (4) The magnetization reversal mechanism is changed from nucleation followed by domain widening to nucleation followed by domain widening and additional nucleation. (5) For the higher ion fluence, deeper buried Co layers are gradually disrupted showing superparamagnetic behaviour.

[1]O. Hellwig, A. Berger, J. B. Kortright, and E. E. Fullerton, J. Magn. Magn. Mater. **319**, 13 (2007).
[2]C. Chappert, H. Bernas, J. Ferré, V. Kottler, J.-P. Jamet, Y. Chen, E. Cambril, T. Devolder, F. Rousseaux, V. Mathet, and H. Launois, Science **280**, 1919 (1998).
[3]A. Mougin, T. Mewes, M. Jung, D. Engel, A. Ehresmann, H. Schmoranzer, J. Fassbender, and B. Hillebrands, Phys. Rev. B **63**, 060409 (2001).
[4]O. Hellwig, D. Weller, A. J. Kellock, J. E. E. Baglin, and E. E. Fullerton, Appl. Phys. Lett. **79**, 1151 (2001).
[5]A. Ehresmann, D. Junk, D. Engel, A. Paetzold, and K. Röll, J. Phys. D **38**, 801 (2005).
[6]A. Ehresmann, D. Engel, T. Weis, A. Schindler, D. Junk, J. Schmalhorst, V. Höink, and G. Reiss, "Fundamentals for magnetic patterning by ion bombardment," Phys. Status Solidi B **243**, 29 (2006).
[7]M. Urbaniak, P. Kuswik, Z. Kurant, M. Tekielak, D. Engel, D. Lengemann, B. Szymanski, M. Schmidt, J. Aleksiejew, A. Maziewski, A. Ehresmann, and F. Stobiecki, Phys. Rev. Lett. **105**, 067202 (2010).
[8]P. Kuswik, A. Ehresmann, M. Tekielak, B. Szymanski, I. Sveklo, P. Maszalski, D. Engel, J. Kisielewski, D. Lengemann, M. Urbaniak, C. Schmidt, A. Maziewski, and F. Stobiecki, Nanotechnology **22**, 095302 (2011).
[9]T. Hauet, O. Hellwig, S.-H. Park, C. Beigné, B. D. Terris, and D. Ravelosona, Appl. Phys. Lett. **98**, 172506 (2011).
[10]J. E. Davies, O. Hellwig, E. E. Fullerton, G. Denbeaux, J. B. Kortright, and K. Liu, Phys. Rev. B **70**, 224434 (2004).
[11]O. Hellwig, G. Denbeau, J. B. Kortright, and E. E. Fullerton, Physica B **336**, 136 (2006).
[12]C. Kooy and U. Enz, Philips Res. Rep. **15**, 7 (1960).
[13]S. Padovani, I. Chado, F. Scheurer, and J. P. Bucher, Phys. Rev. B **59**, 11887 (1999).